Abstract

We present a new tracking algorithm and its implementation called SIMPA. It has the unique feature of long-term tracking of charged particles in arbitrary static electromagnetic fields in a symplectic way. It is relevant to beam dynamics and optics studies whenever the usual hard-edge model cannot describe the accelerator elements accurately or the beamline contains complex magnetic or electric fields. Such a situation arises in the ELENA machine at CERN and many other rings containing an electron cooler. The magnetic field of the electron cooler has a significant influence on the beam dynamics. Frequency analysis and dynamics aperture studies in ELENA are presented with the electron cooler magnetic field included.

DYNAMIC APERTURE AND FREQUENCY ANALYSIS IN ELENA WITH ELECTRON COOLER MAGNETIC FIELD INCLUDED

Lajos Bojtár, CERN Beams Departement

INTRODUCTION

Long-term tracking of charged particles is a fundamental problem of accelerator physics, plasma physics, and it is important in astrophysics. In earlier papers [1, 2] we described a new algorithm allowing long-term symplectic integration of charged particle trajectories in arbitrary static magnetic and electric fields. The approach to particle tracking we described naturally includes the end fields for all kinds of magnets and special elements, like the magnetic system of an electron cooler, with the same treatment. The aim of this paper is to introduce the SIMPA algorithm and software [3] to the cooling expert community. The beam dynamics studies made on the Extra Low ENergy Antiproton (ELENA) ring [4] with SIMPA can be applied to other rings.

THE SIMPA ALGORITHM

We recommend reading the previous papers [1,2] to understand the algorithm in detail, as only a summary is provided here.

Symplectic integrators keep the conserved quantities bounded, but cannot cure the errors coming from the representation of the fields. These are two separate sources of errors. It is crucial to have a physically valid representation of the fields obeying Maxwell's equations close to machine precision, otherwise there is a spurious energy drift during the tracking. This requires a continuous description of the electromagnetic fields in the entire beam region without any cuts. This is an important difference between SIMPA and other tracking codes which usually make element by element tracking and do not handle the electromagnetic field of the ring or beam line as a whole.

The modified surface method

Surface methods describe the fields on the boundary surrounding the region of interest. Field values on the surface determine the magnetic or electric fields in a source-free region. This is true because these fields are harmonic functions satisfying the Laplace equation which has a unique solution for a given boundary condition.

As a first step, the potentials are expressed analytically in terms of point sources. Sources are placed outside the volume of interest, at some distance above the boundary, and their strength is calculated by a system of linear equations such that they reproduce the magnetic or electric field at the boundary. In case of a static electric field, electric point sources are used, since the normal component of the field on the boundary surface is sufficient to describe the field inside the volume. For a static magnetic field this is not always true [1]. For example a field of a solenoid coil can not be reproduced by magnetic monopoles. In early versions of SIMPA, additionally to the magnetic monopoles, current loops were also used. This approach however has several drawbacks. Dirac's magnetic monopoles has singularities which must be directed such, that they do not intersect the volume of interest. The Dirac string singularities also prevent using the Fast Multipole Method [5] for the calculation of field maps. For these reasons the magnetic monopoles recently has been replaced by current point sources. These are two infinitesimally small wires perpendicular to each other and parallel to the boundary surface. Instead of the normal component, two tangential component are matched to the given magnetic field. This modification doubles the number of unknowns to be solved in the resulting linear system of equations, but allows the use of the Fast Multipole Method and eliminates the problem with the Dirac strings and current loops. The Fast Multipole Method can also be used to accelerate the iterative solver, largely compensating for the bigger number of variables.

The relative precision of the reproduction of the magnetic field is typically about 10^{-3} using 10^4 sources for a magnet with length of 1 meter. The precision can be made better by increasing the number of point sources. Regardless of the error relative to the reference field, the reconstructed field is continuous and satisfy Maxwell's equations close to machine precision anywhere inside the volume of interest. This is a key feature of the SIMPA algorithm, and it is the reason of the reconstruction of the field with point sources.

The distance of the point sources from the surface is a free parameter, but it must be chosen carefully. The elevation should be such, that the point sources are not too close to the boundary surface of the element, because the point sources can not be inside the balls of the cover or too close to them. When the sources are too close to the balls, the field expansion will require higher degree spherical harmonics which will make the field map slower and bigger or even impossible to achieve the required level of discontinuity between the balls, which should be in the order of $B_{max} \times 10^{-10}$ or smaller for long-term tracking. On the other hand, when the sources are too far from the boundary surface, the solving of the strengths of the point sources will be difficult, the matrix describing the linear system of equations will be ill-conditioned. As a rule of thumb, the elevation should be about the same as the distance between the points on the boundary surface.

After the potentials are reproduced at the boundary by the point sources, they can be evaluated analytically anywhere inside the volume. However, this method is too slow to be practical.

Solid harmonics

Several orders of magnitude speed improvement can be achieved by using a local description of the potentials. The value of the potentials can be evaluated inside a sphere with radius R with the following expression. In fact, this is the well known formula for regular real solid harmonics inside a unit ball, scaled by R.

$$f(r,\theta,\phi) = \frac{1}{R}\sum_{\ell=0}^{\ell_{max}}\sum_{m=-\ell}^{\ell} r^{\ell}\, c_{\ell m}\, \tilde{P}_{\ell}^{m}(\cos\theta)\, \Phi(\phi;m) \quad (1)$$

We denoted the ϕ dependent part as $\Phi(\phi;m)$ given by

$$\Phi(\phi;m) = \begin{cases} \sqrt{2}\sin(|m|\phi) \text{ if } m < 0 \\ 1 \text{ if } m = 0 \\ \sqrt{2}\cos(m\phi) \text{ if } m > 0 \end{cases} . \quad (2)$$

In the expression above, $\tilde{P}_{\ell}^{m}(\cos\theta)$ is the orthonormalized associated Legendre polynomial, given as:

$$\tilde{P}_{\ell}^{m}(\cos\theta) = \sqrt{\frac{(2\ell+1)}{4\pi}\frac{(\ell-|m|)!}{(\ell+|m|)!}}\, P_{\ell}^{m}(\cos\theta). \quad (3)$$

$P_{\ell}^{m}(\cos\theta)$ is calculated without the Condon-Shortley phase.

In Eq.(1), $r = |\mathbf{r_e} - \mathbf{r_c}|/R$ is the scaled distance between the sphere center $\mathbf{r_c}$ and the evaluation point $\mathbf{r_e}$.

The real-valued coefficients $c_{\ell m}$ are pre-calculated by the following integral:

$$c_{\ell m} = \int_{\mathbf{S}^2} \varphi(\theta,\phi)\, \tilde{P}_{\ell}^{m}(\cos\theta)\, \Phi(\phi;m)\, d\Omega, \quad (4)$$

where $\varphi(\theta,\phi)$ is the potential to be approximated, and $\mathbf{S}^2$ denotes the surface of the sphere. There are several ways to do this integration. An elegant one is, to sum values $\varphi(\theta,\phi)$ on the surface of the sphere at the t-design points with equal weights. A spherical t-design is a set of N points on the sphere, such that a quadrature with equal weights using these nodes is exact for all spherical polynomials of degree at most t. More on t-designs can be found in [6]. An advantage of integrating on a sphere with t-designs is that the sample points have a uniform distribution, contrary to the often used Gaussian quadrature, which has a denser sampling around the poles. As [7] points out, when the sampling points are distributed uniformly on the sphere, the error in the integral is minimized, assuming the errors in the sample values have a normal distribution.

For a set of N points $\{\mathbf{x_i}\}$ in a t-design the following expression is exactly true for all spherical polynomials of maximum degree t or below.

$$\int_{\mathbf{S}^2} \varphi(\mathbf{x}) d\Omega = \frac{4\pi}{N}\sum_{i=0}^{N-1} \varphi(\mathbf{x_i}). \quad (5)$$

Combining Eqns.(4, 5), the spherical harmonics coefficients can be calculated with the following sum:

$$c_{\ell m} = \frac{4\pi}{N}\sum_{i=0}^{N-1} \varphi(\mathbf{x_i})\, \tilde{P}_{\ell}^{m}(\cos\theta(\mathbf{x_i}))\, \Phi(\phi(\mathbf{x_i});m), \quad (6)$$

where N is the number of quadrature points in the t-design. The spherical coordinates $\theta(\mathbf{x_i})$ and $\phi(\mathbf{x_i})$ are expressed in terms of the vectors $\mathbf{x_i}$ pointing to the quadrature points. The author of [6] has published a set of files containing t-designs up to degree 325 on his website for download. A subset of these files has been used in our implementation.

Regular solid harmonics are the canonical representation for harmonic functions inside a sphere. A key characteristic of the algorithm is the description of vector and scalar potentials by solid harmonics inside a set of overlapping spheres covering the volume of interest.

The potentials satisfy exactly the Laplace equation inside the spheres. The discontinuity between the spheres decrease exponentially with the degree of solid harmonics expansion and can be easily kept close to machine precision. The representation of the potentials in terms of solid harmonics is optimal in terms of memory and allows fast evaluation.

Field map preparation

1. The workflow starts with modeling individual magnets with CAD software or measurement data.

2. The strengths of the point sources are calculated for each type of magnet as described earlier.

3. The next step is to assemble the sources according to the lattice of the machine. This is done by rotating and translating the collections of sources to the correct place.

4. The boundary of the volume of interest is described by a Standard Tessellation Language (STL) file. SIMPA provides functionality to create the STL files to describe the beam region. It also can be taken from CAD models.

5. Next, the beam region is filled with overlapping spheres, such that the entire beam region is covered without gaps. For simple beam lines with uniform aperture a single line of spheres is often sufficient. For more complicated geometries HCP lattice is recommended. It leads to several times faster field maps [2]. The spheres should be small enough to not overlap with the sources. The coordinates of the sphere centers on an infinite HCP lattice can be obtained by three simple expressions. Only those spheres are kept from the infinite lattice which are necessary to cover the beam region. Figure 1 shows the ELENA beam region and the centers of the covering spheres. The radius of the spheres was 1 cm in this study and about 76000 of them were needed to cover the beam region of ELENA.

6. The magnets of the beam line or ring are organized into magnet groups. Usually, a magnet group consists of magnets connected to the same power supply.

7. For each magnet group, a field map is produced by calculating the solid harmonics coefficients in each ball in the cover. These field maps are scaled individually, then combined into a global field map. A global field

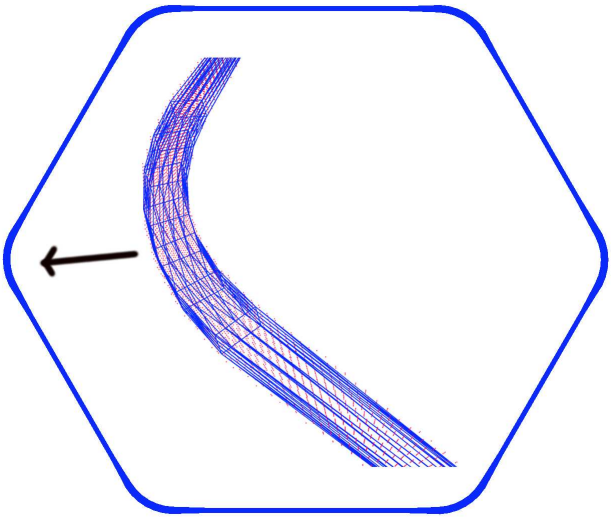

Figure 1: Triangulated boundary of the ELENA beam region. The interior plot is an expanded 3D view of an arc. The red dots are the centers of the covering spheres located on an HCP lattice.

map is a scaled superposition of group field maps. All magnet group field maps are calculated using the same ball cover to allow efficient calculation of their superposition.

Once a global field map is prepared as described above, symplectic tracking can be performed. The motion of a charged particle calculated by the usual relativistic Hamiltonian

$$H = \sqrt{m^2c^4 + c^2(\mathbf{p} - q\mathbf{A})^2} + qV_E, \tag{7}$$

where $\mathbf{A}$ is the vector potential, V_E is the electric scalar potential, $\mathbf{p}$ is the canonical momentum and q is the charge of the particle.

Integrating these equations with classical methods like the Runge-Kutta introduces errors, like the drift of energy or non-preservation of phase-space volume. Symplectic integration methods don't suffer from these problems.

An explicit second-order method for general Hamiltonians, symplectic in extended phase space, is described in [8]. We implemented this integrator, which has the correct long-time behavior.

FREQUENCY ANALYSIS

The method

The drift in the tunes can serve as an early indicator of the long-term stability of the motion [9]. For initial conditions corresponding to chaotic trajectories, the frequency can only be defined for a given time interval. Calculating this local frequency for two consecutive time intervals and taking their difference we can calculate tune shifts $\Delta Q_{h,v}$. For a coasting beam, the figure of merit can be defined as:

$$D = log_{10}(\sqrt{\Delta Q_h^2 + \Delta Q_v^2}) \tag{8}$$

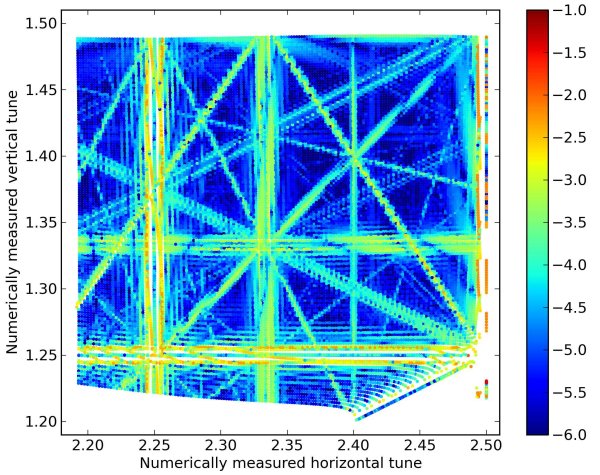

Figure 2: D plotted as colors against the numerically measured tunes for the bare ELENA machine, consisting of only the main bendings and the three quadrupole families.

D calculated with this definition can be used to identify stable areas in the tune diagram.

The tunes were scanned in 160 steps in both directions giving 25600 initial conditions. Each particle was tracked for 300 turns and the phase space variables were saved at a single longitudinal position for each turn. The tracking result is post-processed with the NAFF algorithm [10]. To calculate $\Delta Q_{h,v}$, we split the 300 turns into two sets. Then the figure of merit D in Eq. (8) was calculated for each point in the diagram and plotted as colors.

Results

Fig. 2 shows the figure of merit D for the bare ELENA machine with bending magnets and quadrupoles only, plotted against the tunes as colors. The exercise was repeated with the magnetic elements of the electron cooler included. Fig. 3 shows the numerically measured tunes with the electron cooler included. Fig. 4 shows the magnetic field of the electron cooler. It is apparent that the magnets of the electron cooler have a significant effect on the beam dynamics. Many resonance lines became stronger and wider and particle losses are more frequent at the strongest resonance lines.

On both plots, many higher-order resonance lines can be seen. It should be emphasized, these resonance lines are present also in a perfectly manufactured, built, and aligned machine. We have not put any imperfections into the model. All the resonance lines are the results of the fringe fields of the bending magnets and the quadrupoles. They are the direct consequence of the geometry of the magnets.

DYNAMIC APERTURE

The dynamic aperture of six working points has been calculated and displayed in Table 1 to compare resonance conditions with a non-resonant case. The selected set of

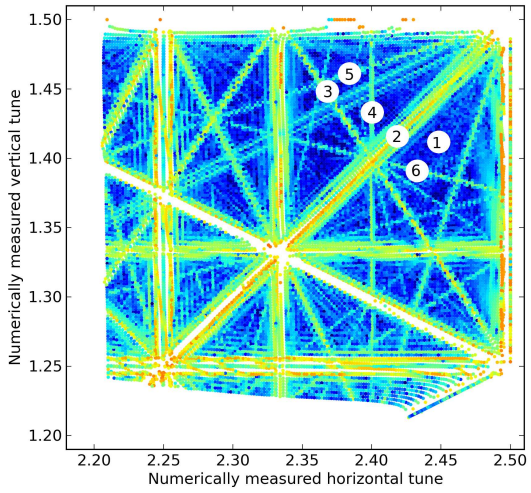

Figure 3: D plotted as colors on the same scale as above against the numerically measured tunes for the ELENA machine with the electron cooler included. The numbered white points in the tune diagram indicate the tunes where the dynamic aperture was calculated.

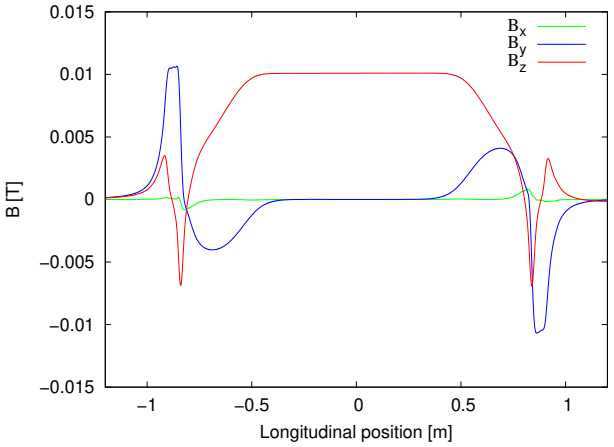

Figure 4: The magnetic field components of the electron cooler plotted against the longitudinal position with transverse coordinates x = y = 2 cm referenced to the design orbit.

tunes is indicated in Fig. 3. These resonance lines were selected because they are close to the region where the working point of ELENA was set during the commissioning. The first working point was chosen to be far from the strong resonance lines at $Q_h = 2.455$, $Q_v = 1.415$. The other five points were placed on resonance lines with various orders.

Stability diagrams are given in Fig. 5 for each point in Fig. 3, which survived $N = 10^4$ turns. In these diagrams, instead of the usual convention of using the physical beam dimensions in units of sigmas of the beam distribution on the axes, we used the single-particle emittances. We did so, because in ELENA, the beam size depends on the perfor-

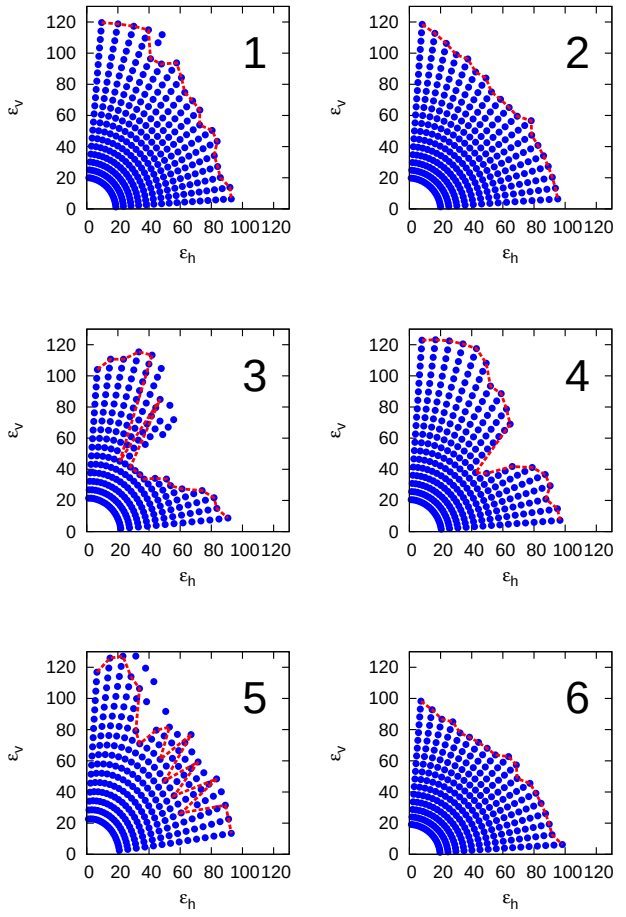

Figure 5: Initial emittances plotted in units of π mm $mrad$ for particle with $dp/p = 0$. Only those initial conditions are plotted which survived $N = 10^4$ turns. The numbers in the upper right corners correspond to the numbering in Fig. 3. The lines indicate the last connected initial emittances for each angle α_k.

Table 1: Dynamic apertures r_d for the six points in Fig. 3 calculated with averaging over the dynamics, see [2]. M is the angular grid size for r_d calculation.

Point	r_d $[m]$	M	Resonance condition
1	0.0115	14	NA
2	0.012	8	$Q_h - Q_v = 1$
3	0.01	6	$3Q_h + 2Q_v = 10$
4	0.0117	3	$5Q_h = 12$
5	0.0113	9	$-Q_h + 3Q_v = 2$
6	0.0113	8	$Q_h + 4Q_v = 8$

mance and duration of the electron cooler, so there is no nominal emittance we could use for comparison.

In Fig. 5 it is apparent that some of the resonance lines make the dynamic aperture significantly smaller than the physical aperture. The transverse acceptance of ELENA is determined by the size of vacuum chambers and the optics.

THE SIMPA SOFTWARE

SIMPA is an open source software written in JAVA for physically valid representation of electromagnetic fields and symplectic tracking. That implies compliance with Maxwell's equations close to machine precision. Symplectic long-term tracking in general electromagnetic fields is a difficult problem and was not fully solved before, to our best knowledge.

At the time of writing the papers [1, 2] the code was experimental and hard to use. Since, the core functionality has been refactored and separated into the 'core' library which can be used for many purposes where a representation of the EM field is needed. The accelerator-specific part was refactored into the 'simpa-acc' package. A command interface was developed, so the user doesn't need to know JAVA programming to set up a simulation. The 'simpa-acc' package has most of the functionality available from the command line interface. Common tasks such as assembling beam lines, tracking particles, calculating optics, matching beam lines are performed with writing text files containing SIMPA commands. Examples are available in the GITLAB source repository [11]. More elaborate tasks such as frequency analysis and dynamical aperture studies described in this paper should use the JAVA API provided. Even in these cases most of the work is done from SIMPA command files and only simple coding is needed.

JAVA used to have a reputation of being slow, however this is not the case anymore. The tracking speed using a single core of an Intel i5-11500 CPU is about 90 turns/seconds in the ELENA machine with 30 meters circumference. It can be further improved using the vector instruction set of the CPU. The vector API is only a preview feature in JDK21, the final implementation comes later.

In the future SIMPA will handle time-varying EM fields at any frequency as well. A number of successful tests has been done aiming in this direction.

CONCLUSIONS

We have applied the SIMPA code for long-term symplectic charged particle tracking in arbitrary static electromagnetic fields on the ELENA machine.

The frequency and dynamic aperture analysis identified a number of 4th and 5th order resonance lines in the tune diagram strong enough to reduce the dynamic aperture below the physical one. What made the frequency and dynamic aperture analyses different, is the fact that we have not introduced any multipole error into our model apart from the multipole components due to the geometry of the magnets, which are inevitable. All the resonances seen in the frequency analysis are direct consequences of the geometry of the fields, even if the magnetic elements are manufactured perfectly.

We showed in the frequency analysis section the effect of the magnetic system of the electron cooler on the beam dynamics by comparing the two cases, with and without electron cooler. The electron cooler introduced non-negligible magnetic perturbations, strengthening many resonance lines. To our best knowledge there was no similar study done before with electron coolers.

REFERENCES

[1] L. Bojtár. Efficient evaluation of arbitrary static electromagnetic fields with applications for symplectic particle tracking. *Nuclear Instruments and Methods A*, 948:162841, 2019.

[2] Lajos Bojtár. Frequency analysis and dynamic aperture studies in a low energy antiproton ring with realistic 3d magnetic fields. *Phys. Rev. Accel. Beams*, 23:104002, Oct 2020.

[3] `https://simpa-project.web.cern.ch/`.

[4] V. Chohan et al. *Extra Low ENergy Antiproton (ELENA) ring and its Transfer Lines: Design Report*. CERN, 04 2014.

[5] V Rokhlin. Rapid solution of integral equations of classical potential theory. *Journal of Computational Physics*, 60(2):187–207, 1985.

[6] R. S. Womersley. Efficient spherical designs with good geometric properties. 2017.

[7] V. I. Lebedev. Quadratures on a sphere. *USSR Computational Mathematics and Mathematical Physics, 16*, 1976.

[8] M. Tao. Explicit symplectic approximation of nonseparable hamiltonians: Algorithm and long time performance. *Phys. Rev. E*, 94:043303, Oct 2016.

[9] E. Todesco, M. Giovannozzi, and W. Scandale. Fast indicators of long term stability. *Particle Accelerators*, 55:27–36, 1996.

[10] J. Laskar. The chaotic motion of the solar system: A numerical estimate of the size of the chaotic zones. *Icarus*, 88(2):266 – 291, 1990.

[11] `https://gitlab.cern.ch/lbojtar/simpa/-/tree/master/examples`.